New Light Shed on Charge Transfer in Fundamental $H^+ + H_2$ Collisions

X. Urbain,[1] N. de Ruette,[2] V. M. Andrianarijaona,[3] M. F. Martin,[3] L. Fernández Menchero,[4] L. F. Errea,[5] L. Méndez,[5] I. Rabadán,[5] and B. Pons[6]

[1]*IMCN, Université Catholique de Louvain, Chemin du Cyclotron 2, 1348 Louvain-la-Neuve, Belgium*
[2]*Columbia Astrophysics Laboratory, Columbia University, 550 West 120th Street, New York, New York 10027, USA*
[3]*Department of Physics, Pacific Union College, Angwin, California 94508, USA*
[4]*Department of Physics, University of Strathclyde, 107 Rottenrow, East Glasgow G4 0NG, United Kingdom*
[5]*Laboratorio Asociado al CIEMAT de Física Atómica y Molecular en Plasmas de Fusión, Departamento de Química, Universidad Autónoma de Madrid, Cantoblanco E-28049 Madrid, Spain*
[6]*CELIA, Université Bordeaux I-CNRS-CEA, 351 Cours de la Libération, 33405 Talence, France*

(Received 7 August 2013; published 12 November 2013)

There is no consensus on the magnitude and shape of the charge transfer cross section in low-energy $H^+ + H_2$ collisions, in spite of the fundamental importance of these collisions. Experiments have thus been carried out in the energy range $15 \leq E \leq 5000$ eV. The measurements invalidate previous recommended data for $E \leq 200$ eV and confirm the existence of a local maximum around 45 eV, which was predicted theoretically. Additionally, vibrationally resolved cross sections allow us to investigate the evolution of the underlying charge transfer mechanism as a function of E.

DOI: 10.1103/PhysRevLett.111.203201 PACS numbers: 34.50.−s, 34.70.+e

Collisions between protons and hydrogen molecules are involved in the physics of many large-scale systems. For instance, the charge transfer reactions $H^+ + H_2 \rightleftharpoons H + H_2^+$ are of great importance for the chemistry and cooling behavior of low-density primordial gas [1]; it accordingly influences the general state and hydrodynamics of the cosmological medium [2]. H_2 molecules, and isotopical variants, are also abundant in the edge region of tokamak devices where the plasma is relatively cold and dense; therefore, their interaction with surrounding ions must explicitly be considered in order to obtain a reliable description of the edge and divertor plasmas [3]. Besides its relevance in astrophysics and fusion research, the collision $H^+ + H_2$ is a fundamental few-body system which constitutes the benchmark for the theoretical description of all ion-molecule collisions. In this Letter we focus on the nondissociative charge transfer (CT) reaction:

$$H^+ + H_2(X^1\Sigma_g^+, \nu = 0) \rightarrow H(1s) + H_2^+(X^2\Sigma_g^+, \nu'), \quad (1)$$

for $E \geq 15$ eV, where nuclear exchange is negligible [4]. ν and ν' are, respectively, the vibrational quantum numbers of H_2 and H_2^+ molecules. In spite of the apparent simplicity of this process, there is considerable disagreement between the existing calculations and measurements. One can note this disagreement by glancing at the results plotted in Fig. 1, where we display the total cross section for reaction (1), obtained by summing over all vibrational exit channels ν', as a function of the collision energy. We deem that this is an unsatisfactory situation for such a basic system, especially for energies below 100 eV.

The main difference between reaction (1) and similar CT processes in ion-atom collisions is the rovibrational motion of the molecular species. At high collision energies, the rotation and vibration periods are large compared to the characteristic collision time. The CT process is thus described in the framework of the Franck-Condon approximation, where the target nuclei remain fixed during the collision. As the energy decreases below 1 keV, this

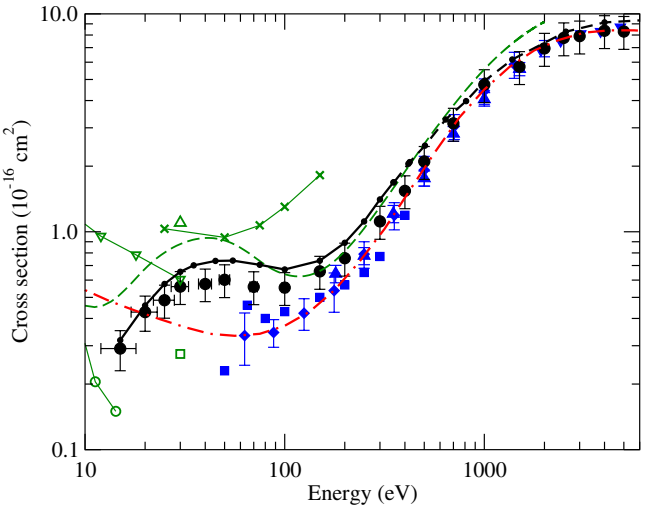

FIG. 1 (color online). Total CT cross sections for $H^+ + H_2$ collisions [reaction (1)], as functions of the collision energy. Present results: (filled circle) experiment; (black solid line with small dot) quantal calculation; (black dashed line with small dot) semiclassical calculation. Previous experiments: (blue filled square) Cramer [15]; (blue filled downward triangle) McClure [16]; (blue filled diamond) Gealy and Van Zyl [17]; (blue filled upward triangle) Kusakabe *et al.* [18]. Recommended data: (red dash-dotted line) Phelps [19]. Previous calculations: (green open upward triangle) Baer *et al.* [9]; (green open square) Morales *et al.* [14]; (green dashed line with open downward triangle) Ichihara *et al.* [13]; (green solid line with open circle) Krstić [10]; (green solid line with crosses) Krstić and co-workers [24]; (green dashed line) nonreactive CT from Ref. [4].

approximation breaks down. A less restrictive description is provided by the sudden vibrational approximation (SVA) [5,6], where it is assumed that the vibrational wave function does not change during the collision. It was shown [7] that SVA calculations and experiments disagree for energies below 200 eV and the failure was traced back to the inability of the SVA to describe the two-step low-energy mechanism of Niedner *et al.* [8]. In the first step of this mechanism, the interaction of the charged projectile with the molecule removes electron density from the target bond ("bond dilution"), modifying the interatomic potential, which leads to the vibrational excitation of H_2. The CT reaction takes place in a second step by transition from H_2 excited vibrational states to quasidegenerate vibrational states of H_2^+. It is clear that the mechanism of reaction (1) involves a subtle interplay between electronic and nuclear degrees of freedom, and the experimental confirmation of the calculations and proposed mechanisms is essential.

In a pioneering work, Baer and co-workers [9] carried out a calculation using the so-called infinite order sudden approximation (IOSA), where the vibrational motion is explicitly considered, at a collision energy $E = 30$ eV. A similar method has been applied in Refs. [10,11] at energies $E < 20$ eV. The calculation of Errea *et al.* [12] employed *ab initio* electronic wave functions and a vibronic basis set within quantal and semiclassical frameworks, covering a large energy range (10 eV $< E <$ 10 keV). Other semiclassical methods, such as trajectory surface hopping [13], electron nuclear dynamics [14], and classical trajectory-diatomics in molecules [4], have also been applied, and the ensuing total cross sections are shown in Fig. 1. As already mentioned, the dispersion of the results for $E < 100$ eV is conspicuous.

Previous measurements of the CT total cross section have been performed by Cramer [15], McClure [16], Gealy and Van Zyl [17], and Kusakabe *et al.* [18]. While the total cross sections obtained in all these experiments are practically identical for $E > 500$ eV, discrepancies at low energies are noticeable. The recommended data of Phelps [19] interpolate between the experimental data of Gealy and Van Zyl [17] for $E > 60$ eV and those of Holliday *et al.* [20] for $E < 5$ eV. Differential measurements have been performed by Niedner *et al.* [8] at 30 eV.

In this work we have measured total and vibrationally resolved CT cross sections for $E = 15$–5000 eV with two aims: first, to obtain state-of-the-art values of the total cross section, which allow us to provide a new set of recommended data, and second, to probe the CT mechanism and underlying interplay of electronic and nuclear motions.

In the experimental setup (Fig. 2), the protons are extracted from a duoplasmatron ion source and accelerated to an energy equal to the sum of the desired collision energy and the voltage applied to the collision region. They are decelerated in a unique combination of einzel lens and resistive glass tube to enter the collision region

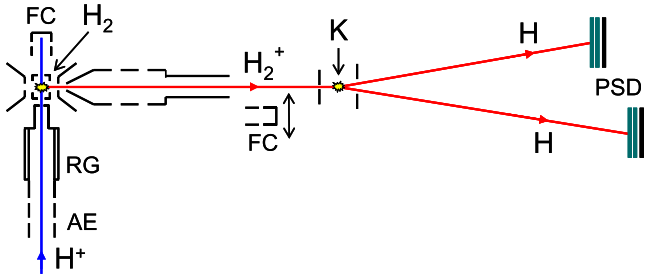

FIG. 2 (color online). Experimental setup (not to scale): AE, assymetric einzel lens; RG, resistive glass tube; FC, Faraday cups; PSD, position sensitive detectors. The H_2 and K targets are effusing from capillaries.

where they cross an effusive jet of H_2, all molecules being in their vibrational ground state. To ensure proper transmission of the proton beam and simultaneous extraction of the daughter ions, a saddle point electrode arrangement is used, which minimizes the transverse electric field on the proton beam axis while producing a focusing extraction geometry in the perpendicular direction. Intensities of the order of 10 nA are routinely achieved down to 15 eV, as measured in a Faraday cup located downstream. The daughter molecular ions are further accelerated to 2 keV as they leave the floating interaction region and are shaped into a beam. Direct measurement of the secondary ion current in the picoampere range together with systematic variation of the density of the gas target allow the determination of relative CT cross sections as a function of energy.

In order to put the proton-H_2 cross sections on an absolute scale, a global scaling factor was determined by comparison with the values of Gealy and Van Zyl [17] between 400 and 2000 eV. The 14% uncertainty (90% C.L.) affecting those measurements has been combined in quadrature with our measurement uncertainty. To evaluate the reliability of the method, a beam of H_2^+ was sent to the H_2 target, and ratios of the beam intensities were measured for the same pressure range under identical experimental conditions. These results, when normalized with the same factor determined for proton-H_2 collisions, perfectly match the recommended cross sections for $H_2^+ + H_2$ symmetric CT [21] between 100 and 1000 eV. Error bars on the collision energy correspond to the energy spread (5 eV FWHM) of our proton source, as measured by collinear Doppler spectroscopy after neutralization on a Cs target.

In order to obtain vibrationally resolved CT cross sections, the product ions are made to cross an effusive potassium jet where they undergo resonant dissociative CT [22]. Because of energy and momentum conservation in the predissociation process, the positions and flight time difference of the two resulting H atoms give access to the vibrational distribution of the CT products. The new experimental total cross sections are plotted in Fig. 1, while measured vibrational branching ratios are shown in Fig. 3.

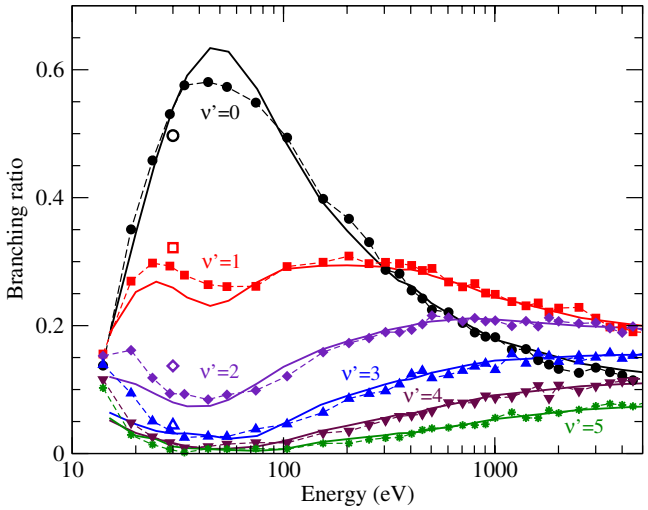

FIG. 3 (color online). Branching ratios for populating the vibrational states of the H_2^+ molecule [Eq. (4)] in the CT reaction (1), as functions of the collision energy. Full lines, theoretical results; dashed lines with symbols, experimental results; open symbols, results of Niedner *et al.* [8].

Earlier measurements of the total cross section all converge to the same value above 500 eV, as do the present experimental results. While we have measured the H_2^+ production, Gealy and Van Zyl [17] measured the neutralization yield, which requires the determination of the secondary emission coefficient and proper angular collection of the scattered hydrogen atoms. This may explain the smaller values they obtained at low energy. The important difference between our measurements and the recommended data of Phelps [19] is a consequence of (i) the difference between our data and those of Ref. [17], which were used to construct the recommended data, and (ii) the emergence of a local maximum in our measurements about $E = 45$ eV, an energy region previously unexplored experimentally.

We have also carried out new calculations using the vibrational-close-coupling method of Ref. [12] with *ab initio* electronic wave functions. In the quantal treatment, the collision wave function is solution of the stationary Schrödinger equation

$$H(\boldsymbol{r}, \boldsymbol{\rho}, \boldsymbol{R})\Psi(\boldsymbol{r}, \boldsymbol{\rho}, \boldsymbol{R}) = E\Psi(\boldsymbol{r}, \boldsymbol{\rho}, \boldsymbol{R}), \quad (2)$$

where E is the collision energy, H is the total Hamiltonian, $\boldsymbol{r}$ denotes the electronic coordinates, $\boldsymbol{\rho}$ is the internuclear vector of the target molecule, and $\boldsymbol{R}$ is the projectile position vector with respect to the center of the H_2 internuclear vector. The collision wave function is expressed as

$$\Psi(\boldsymbol{r}, \boldsymbol{\rho}, \boldsymbol{\xi}) = \sum_n \sum_\nu F_{n\nu}(\boldsymbol{\xi})\phi_n(\boldsymbol{r}; \rho, \boldsymbol{\xi})\chi_{n\nu}(\rho), \quad (3)$$

where $\boldsymbol{\xi}$ is a reaction coordinate, combination of $\boldsymbol{R}$ and $\boldsymbol{r}$, built so as the boundary conditions are correctly fulfilled (see [12]). The vibronic basis $\{\phi_n\chi_{n\nu}\}$ is formed by products of the electronic functions ϕ_n and the vibrational functions $\chi_{n\nu}$. Our basis set includes the two lowest electronic states of H_3^+ and a vibrational basis of 35 states for both H_2 and H_2^+. A critical point in the calculation is the appropriate description of the conical intersection between the ground and first potential energy surfaces (PESs) of H_3^+, found in the limit $R \to \infty$ at $\rho \approx 2.45$ bohr. While transitions near this intersection are important in the CT reaction, the calculation cannot be performed using the adiabatic electronic states, which are coupled by singular nonadiabatic couplings. In practice, we use a couple of "regularized" states, obtained through a unitary transformation of the adiabatic functions.

The rotation of the diatomic molecules is described within the IOSA framework: the molecule orientation is kept fixed during the collision; this is justified for $E \geq 15$ eV, where the characteristic collision time is ≈ 12 fs and the H_2 rotation period ≈ 1 ps. Accordingly, the wave function (3) does not include a rotational component. However, H depends on the relative orientation of vectors $\boldsymbol{\rho}$ and $\boldsymbol{R}$; in the IOSA treatment, the angle $\alpha = \arccos(\hat{\boldsymbol{\rho}} \cdot \hat{\boldsymbol{R}})$ is treated as a parameter that does not vary during the collision, and the Schrödinger equation is solved for several values of this parameter. In this treatment the Coriolis couplings, due to the rotation of $\boldsymbol{R}$ in the laboratory frame, are neglected. The cross section presented in Fig. 1 is finally obtained by averaging over α.

At high energies, we use a semiclassical (eikonal) method, where the vector $\boldsymbol{R}$ follows rectilinear trajectories. The dynamics is still described in terms of the vibronic $\phi_n\chi_{n\nu}$ states. However, the Coriolis couplings are no longer neglected, in contrast to the quantal case.

The results of our calculations are also included in Fig. 1, where we plot the results obtained by means of the quantal treatment for $E < 350$ eV, and those from the semiclassical calculation for $E > 350$ eV. We have checked that both methods lead to identical total and partial cross sections in the energy range $200 < E < 400$ eV. At $E < 200$ eV, trajectory effects start to be sizable and the eikonal calculation is inaccurate. For $E > 350$ eV, trajectory effects are negligible and the eikonal result is somewhat more accurate than its quantal counterpart (the differences are of the order of 10% at $E = 1$ keV) because the Coriolis couplings are relevant.

As demonstrated by Fig. 1, our experimental and theoretical results fall in excellent agreement over the whole energy range. The calculated values are essentially those presented in Ref. [12] (not shown in the figure), although the new cross section is somewhat lower (by $\approx 25\%$) than the previous one for $E < 100$ eV; this change is due to an improvement of the regularization of the conical intersection at small α, which shows the sensitivity of the cross section to the details of the PESs. In this respect, previous IOSA calculations [9,10] differ either by the use of approximate PESs or by the approximations made in the regularization procedure.

We find a qualitative agreement with the cross section for nonreactive CT of Ref. [4]. In that work, the electron dynamics was described in terms of approximate diatomics-in-molecules wave functions [23] and the nuclear motion was restricted to the fundamental PES; this restriction is not fully consistent with the CT dynamics, where the electron jumps on the excited PESs, and this mainly explains the overestimation observed in Fig. 1. Besides intrinsically different treatments of the electron dynamics, the disagreement between our results and previous calculations (electron nuclear dynamics [14], trajectory surface hopping [13], and semiclassical IOSA [24]) also points to the necessity to quantally describe the nuclear motion for $E < 200$ eV.

Our experimental setup does not enable us to access the dissociative part of the CT process. However, the excellent agreement between the measured and computed nondissociative CT component (Fig. 1) provides a confirmation of the present calculations which indicate that the dissociative CT cross section never exceeds 1% of the total CT one for $15 \leq E \leq 5000$ eV, while nuclear exchange is also negligible.

We now turn our attention to the CT mechanism encoded in the state-resolved vibrational cross sections. The comparison of experimental and theoretical vibrational cross sections is plotted in Fig. 3, where we display the branching ratios

$$r_{\nu'}(E) = \frac{\sigma^{\mathrm{CT}}_{\nu'}(E)}{\sigma^{\mathrm{CT}}(E)}. \tag{4}$$

$\sigma^{\mathrm{CT}}_{\nu'}$ is the integral cross section for populating the state $H_2^+(X^2\Sigma_g^+, \nu')$ in reaction (1) and σ^{CT} is the total CT cross section. One can note the very good agreement between theory and experiment that provides a stringent test of the methods. We have also included in this figure the results of Niedner *et al.* [8] at $E = 30$ eV, which satisfactorily agree with our measurements.

Our calculations basically confirm that, for $E \lesssim 200$ eV, CT reactions take place through transitions from excited vibrational states of H_2 to vibrational states of H_2^+ on the way out of the collision. Direct transitions from the $H^+ + H_2(X^1\Sigma_g^+, \nu = 0)$ entry state to the $H(1s) + H_2^+(X^2\Sigma_g^+, \nu')$ capture states are indeed inhibited because of the large energy gap between these channels, while the $H^+ + H_2(X^1\Sigma_g^+, \nu \geq 4)$ excitation states lie close in energy to the $H(1s) + H_2^+(X^2\Sigma_g^+, \nu' \geq 0)$ capture ones. Among the available $\nu \rightarrow \nu'$ transitions, $\nu = 4 \rightarrow \nu' = 0$ is the most efficient since (i) primary vibrational excitation leads to $H_2(X^1\Sigma_g^+, \nu)$ populations that decrease as ν increases [4], and (ii) the excitation $H^+ + H_2(X^1\Sigma_g^+, \nu = 4)$ and capture $H(1s) + H_2^+(X^2\Sigma_g^+, \nu' = 0)$ channels are asymptotically quasidegenerate. Therefore, $H_2^+(X^2\Sigma_g^+, \nu' = 0)$ is the most populated CT exit channel at low E.

As E increases, the effective collision time becomes shorter, which leads to sudden transitions where capture occurs through vertical transitions from the $H_2(X^1\Sigma_g^+, \nu = 0)$ entrance channel. The relative populations of the $H_2^+(X^2\Sigma_g^+, \nu')$ states become independent of E and proportional to the Franck-Condon factors, $\gamma_{0\nu'} = |\langle\chi_0|\chi_{\nu'}\rangle|^2$. Since $\gamma_{02} > \gamma_{01} > \gamma_{00}$, we accordingly expect $r_{\nu'=2} > r_{\nu'=1} > r_{\nu'=0}$. This tendency can be observed in Fig. 3.

The shape of $r_{\nu'=0}$ shows a maximum at $E \approx 45$ eV, the same energy where the total CT cross section of the Fig. 1 curve has a local maximum. It is noteworthy that the cross section for the vibrational excitation $\nu = 0 \rightarrow \nu = 4$, which is involved in the two-step CT process through $H_2(X^1\Sigma_g, \nu = 0) \rightarrow H_2(X^1\Sigma_g^+, \nu = 4) \rightarrow H_2^+(X^2\Sigma_g, \nu' = 0)$, also presents a maximum in the same energy region [12,25]. Furthermore, the most important transitions $\nu = 4 \rightarrow \nu' = 0$ take place near the avoided crossing of the $H^+ + H_2(X^1\Sigma_g^+, \nu = 4)$ and $H(1s) + H_2^+(X^2\Sigma_g^+, \nu' = 0)$ states about $R = 6$ a.u. When E decreases, these transitions become inefficient because the pseudocrossing energy gap becomes prohibitive. Other (more narrow) avoided crossings then play a significant role: for example, the transition in the avoided crossing between the states dissociating into $H^+ + H_2(X^1\Sigma_g^+, \nu = 5)$ and $H(1s) + H_2^+(X^2\Sigma_g^+, \nu' = 1)$ populates this channel, leading to a maximum in the corresponding partial cross section at $E \approx 25$ eV. However, since the population of the $\nu = 5$ excitation channel is smaller than that of the $\nu = 4$ state, this mechanism does not compensate the fall of the population of the $\nu' = 0$ state, resulting in a decrease of the total CT cross section of Fig. 1.

In conclusion, we have presented vibrationally resolved measurements of CT cross sections for the fundamental $H^+ + H_2$ system in a wide impact energy range from 15 to 5000 eV. Our total cross section measurements invalidate the previous recommended data [19] for $E < 200$ eV. This has significant consequences for all forthcoming experiments which would use CT in $H^+ + H_2$ for normalization purposes. We have performed vibronic-close-coupling calculations, which have yielded results in excellent agreement with the present experiments, for both total and vibrationally resolved cross sections. This has allowed us to study the evolution of the CT mechanism with the collision energy. For $E \leq 200$ eV, there is a strong interplay between dynamical nuclear and electronic degrees of motion. This marks the lower energy bound of accuracy of the nuclear sudden approximations commonly used in the theoretical description of more complex ion-molecule collisions.

We acknowledge financial support from Project No. ENE2011-28200 (Secretaría de Estado de I + D + i, Spain), the F. R. S.-FNRS under I. I. S. N. Contract No. 4.4504.10, the Association Euratom-Belgian State, and the National Science Foundation under Grant No. PHY-1068877.

[1] T. Abel, P. Anninos, Y. Zhang, and M. L. Norman, New Astron. **2**, 181 (1997).
[2] P. Anninos, Y. Zhang, T. Abel, and M. L. Norman, New Astron. **2**, 209 (1997).
[3] http://www-amdis.iaea.org/CRP/HydrogenHelium/public.html.
[4] L. F. Errea, C. Illescas, A. Macías, L. Méndez, B. Pons, I. Rabadán, and A. Riera, J. Chem. Phys. **133**, 244307 (2010).
[5] V. Sidis, Adv. At., Mol., Opt. Phys. **26**, 161 (1989).
[6] L. F. Errea, J. D. Gorfinkiel, A. Macías, L. Méndez, and A. Riera, J. Phys. B **30**, 3855 (1997).
[7] L. F. Errea, A. Macías, L. Méndez, I. Rabadán, and A. Riera, Phys. Rev. A **65**, 010701(R) (2001).
[8] G. Niedner, M. Noll, J. P. Toennies, and C. Schlier, J. Chem. Phys. **87**, 2685 (1987).
[9] M. Baer, G. Niedner-Schatteburg, and J. P. Toennies, J. Chem. Phys. **91**, 4169 (1989).
[10] P. S. Krstić, Phys. Rev. A **66**, 042717 (2002).
[11] P. S. Krstić and R. K. Janev, Phys. Rev. A **67**, 022708 (2003).
[12] L. F. Errea, L. Fernández, L. Méndez, B. Pons, I. Rabadán, and A. Riera, Phys. Rev. A **75**, 032703 (2007).
[13] A. Ichihara, O. Iwamoto, and R. Janev, J. Phys. B **33**, 4747 (2000).
[14] J. Morales, A. Diz, E. Deumens, and Y. Öhrn, J. Chem. Phys. **103**, 9968 (1995).
[15] W. H. Cramer, J. Chem. Phys. **35**, 836 (1961).
[16] G. W. McClure, Phys. Rev. **148**, 47 (1966).
[17] M. W. Gealy and B. I. Van Zyl, Phys. Rev. A **36**, 3091 (1987).
[18] T. Kusakabe, L. Pichl, R. J. Buenker, M. Kimura, and H. Tawara, Phys. Rev. A **70**, 052710 (2004).
[19] A. V. Phelps, J. Phys. Chem. Ref. Data **19**, 653 (1990).
[20] M. G. Holliday, J. T. Muckerma, and L. Friedman, J. Chem. Phys. **54**, 1058 (1971).
[21] C. F. Barnett, Oak Ridge National Laboratory Technical Report No. ORNL-6086 A-58, 1990.
[22] X. Urbain, B. Fabre, E. M. Staicu-Casagrande, N. de Ruette, V. M. Andrianarijaona, J. Jureta, J. H. Posthumus, A. Saenz, E. Baldit, and C. Cornaggia, Phys. Rev. Lett. **92**, 163004 (2004).
[23] F. O. Ellison, J. Am. Chem. Soc. **85**, 3540 (1963).
[24] P. S. Krstić *et al.*, http://www-cfadc.phy.ornl.gov/h2mol.
[25] W. R. Gentry and C. F. Giese, Phys. Rev. A **11**, 90 (1975).